The Higher the Better? Hedging and Investment Strategies in Cryptocurrency Markets: Insights from Higher Moment Spillovers

Xie He
Shigeyuki Hamori

September 2023

Discussion Paper No. 2315

GRADUATE SCHOOL OF ECONOMICS

KOBE UNIVERSITY

ROKKO, KOBE, JAPAN

The Higher the Better? Hedging and Investment Strategies in Cryptocurrency Markets: Insights from Higher Moment Spillovers

Xie He
Graduate School of Economics, Kobe University
2-1, Rokkodai, Nada-Ku, Kobe 657-8501 JAPAN

Shigeyuki Hamori (corresponding author)
Graduate School of Economics, Kobe University
2-1, Rokkodai, Nada-Ku, Kobe 657-8501 JAPAN
Email: hamori@econ.kobe-u.ac.jp

Abstract

This study aims to investigate whether conditional higher moments offer additional and distinct information compared to lower moments in spillover effect analysis, and to examine their relevance for portfolio construction and hedging strategies. We employ the autoregressive conditional density (ACD) model to estimate the conditional skewness and kurtosis of nine major cryptocurrency markets. Furthermore, we explore the higher moment spillovers among these markets using the Diebold Yilmaz spillover approach. The results confirm that the magnitude and direction of spillover effects vary across different moments in the cryptocurrency market, each providing unique insights. Additionally, we find that although the spillover effects exhibit variations over different time periods and market conditions, the skewness spillover and kurtosis spillover, which track the transmission of downside (upside) risk and tail risk respectively, demonstrate similarities in their patterns. These variations differ noticeably from the changes observed in volatility spillover, which tracks the transmission of volatility risk. Finally, comparing the minimum connectedness portfolio (MCoP) based on different moment spillovers, we discover that the MCoP derived from higher moment spillovers exhibits superior hedge effectiveness and Sharpe ratios.

Key words: Higher moments; Spillover effect; Cryptocurrency markets
JEL classification: G15; F3; C32
Funding: This work was supported by JSPS KAKENHI Grant Number 22K01424

1. Introduction

The spectacular collapse of the US housing market and the bursting of the US mortgage bubble in the summer of 2007 directly triggered a severe financial crisis in 2008. This crisis begins in the US stock market and spreads rapidly to other financial sectors. The crisis spreads to other countries, transforming a local crisis into a global one. This event serves as a reminder to closely monitor spillover effects between markets to prevent shocks from one market from spreading to others.

Numerous techniques can be utilized to measure spillover effects. Some of the commonly employed techniques include vector autoregression (VAR) models, multivariate generalized autoregressive conditional heteroskedasticity (M-GARCH) models such as dynamic conditional correlation (DCC) GARCH, and Copula Models. In recent years, the Diebold Yilmaz connectedness (spillover) approach has garnered increasing attention from researchers. It measures the spillover effect in the generalized VAR framework and was first proposed by Diebold & Yilmaz (2009). It quantifies both the strength and direction of spillover effects within a fixed investment horizon.

Based on the Diebold Yilmaz connectedness approach, an extensive amount of literature has investigated the spillovers of returns and volatilities (e.g., Diebold & Yilmaz, 2009; He et al., 2020; Liu & Hamori, 2020; Sun et al., 2022; Tiwari et al., 2018). Since returns and volatilities track changes in investor expectations and market volatility risks, return spillover and volatility spillover are considered to track inter-market expectational links and volatility risk links (Diebold & Yilmaz, 2015). Recently,

researchers have started extending spillover analysis to higher moments, such as skewness and kurtosis. Skewness and kurtosis of returns are considered to measure downside (upside) risk or tail risk in challenging times and under adverse scenarios in financial markets (He & Hamori, 2023). Compared with volatility spillover, skewness spillover and kurtosis spillover can capture extreme tail co-movements between markets. Higher moment spillovers can effectively detect some important events that may not be effectively captured by return and volatility spillover (Bouri et al., 2021).

Similar to volatility, both skewness and kurtosis are latent and need to be estimated. Several higher moment spillover analyses based on realized measures or model-based estimates have garnered attention (e.g., Finta and Aboura 2020; Gkillas et al. 2022; He and Hamori 2021; Nekhili and Bouri 2023; Zhang et al. 2022). One major advantage of realized measures is their ease of calculation, and therefore, most of the literature on higher moment spillover has utilized realized measures. However, model-based estimates allow for more sophisticated and flexible modeling techniques, such as the autoregressive conditional density (ACD) model and GARCHSK models. These models capture the conditional dependencies and dynamics in the data, providing more accurate and robust volatility estimates. Additionally, model-based estimates of skewness or kurtosis do not require high-frequency data, unlike realized measures, which rely on high-frequency data. He and Hamori (2021) conducted pioneering work in spillover analysis of conditional higher moments. They focused on major global stock markets as the subject of their study and employed the ACD model to estimate

their conditional higher moments, obtaining robust results in the stock market and confirming the importance of measuring higher order spillover effects.

In recent years, cryptocurrencies like Bitcoin and Ethereum have gained increasing prominence, reshaping the financial landscape and disrupting conventional understandings of currency. They have opened up new opportunities for investment and financial transactions. Cryptocurrencies have emerged as a noteworthy financial asset class, displaying distinct features, market structure, price determinants, risk factors, and regulatory considerations in contrast to traditional financial products. Given the significance and distinctive nature of the cryptocurrency market, we incorporate high moment spillover analysis into our study. This approach allows us to examine the similarities and differences in high moment spillover effects between cryptocurrencies and other markets.

The Diebold Yilmaz connectedness approach has long been considered to provide important information for practical investment decisions, but its specific application remains a widely discussed issue. However, in recent times, it has found practical application in portfolio construction. Broadstock et al. (2020) introduced a portfolio technique called the Minimum Connectedness Portfolio (MCoP). This approach aims to construct a portfolio by minimizing interconnectedness and spillover effects among investment assets. Several studies related to the MCoP have confirmed the significant role played by return connectedness or volatility connectedness in portfolio construction (e.g., Abdullah, Chowdhury, and Sulong 2023; Adekoya et al. 2022; Cui

and Maghyereh 2023; Tiwari et al. 2021). Additionally, the MCoP has exhibited favorable financial performance for certain financial assets. However, there is limited literature on MCoP based on higher moment connectedness. The applicability of higher moment connectedness to this strategy, as well as its role in hedging strategies and portfolio construction, still need to be verified.

For these reasons, we follow the approach of He & Hamori (2021) and estimate the conditional skewness and kurtosis using the ACD model. Subsequently, we extend the Diebold-Yilmaz connectedness approach to incorporate higher moments. We investigate the spillover of skewness and kurtosis among 9 major cryptocurrencies, analyzing their implications for the transmission of downside (upside) risk and tail risk. Furthermore, we examine the role of skewness spillover and kurtosis spillover in portfolio construction, assessing whether the MCoP based on higher moment connectedness exhibits superior hedge effectiveness compared to that based on volatility connectedness. To the best of our knowledge, this paper represents the first research endeavor to explore the spillover effects of conditional higher moments across cryptocurrency markets. Moreover, it contributes to the existing literature by investigating the role of higher moment spillovers in hedging strategies and portfolio construction.

Here are some major findings of this paper:

First, we find that the total spillovers across cryptocurrency markets decrease as the order of the moment increases. The total skewness spillover and total kurtosis

spillover are smaller than the total volatility spillover among all markets. Additionally, the changes in skewness and kurtosis spillovers display high similarity, implying a consistent pattern in the transmission of downside (upside) risk and tail risk across markets over time. However, the changes and fluctuations in downside (upside) risk and tail risk are notably different from the transmission patterns of volatility risk.

Second, for each cryptocurrency, the spillover from and to other cryptocurrencies varies across different moments. Binance Coin (BNB) and Bitcoin (BTC) dominate in transmitting volatility and kurtosis, respectively, while Cardano (ADA) exhibits the highest skewness spillover transmitted to others.

At last, to examine whether higher-moment spillovers can be used in portfolio construction and hedging strategies, we introduce the higher moment connectedness into the MCoP and explore the historical investment performance of them through back-testing.

We find that compared to the MCoP based on volatility, the MCoP based on higher moments shows better hedge effectiveness and higher Sharpe ratios for volatility, Value at Risk (VaR), and expected shortfall (ES). Particularly, in terms of hedge effectiveness and Sharpe ratios, the Minimum Connectedness Portfolio (MCoP) based on kurtosis connectedness and skewness connectedness demonstrates the best performance, respectively.

The remainder of this paper is organized as follows. Section 2 presents the empirical methods, including the ACD model, the Diebold Yilmaz TVP-VAR-based

connectedness approach, and a novel portfolio technique named MCoP. Section 3 describes the data, reports the summary statistics, and presents the results of the tests. The results are discussed in Section 4, and Section 5 provides a summary and conclusions.

2. Methodology

2.1. The Autoregressive Conditional Denity Model

To capture the dynamic behavior of higher moments, such as skewness and kurtosis, Hansen (1994) introduced the Autoregressive Conditional Density (ACD) model, which generalizes GARCH type dynamics to time varying conditional higher moments and such subsumes them.

A first order constant-GARCH(1,1) model with general ACD dynamics can be written as:

$$r_t = \mu_t + \epsilon_t = \mu_t + \sigma_t z_t, \tag{1a}$$

$$\sigma_t^2 = \omega + \alpha_1 \epsilon_{t-1}^2 + \beta_1 \sigma_{t-1}^2. \tag{1b}$$

where ϵ_t is the innovation, and z_t is white noise and assumed to follow some appropriately distribution $\mathfrak{D}(0,1,\rho_t,\zeta_t)$[1]. ρ_t and ζ_t are skew parameter and shape parameter, which control the asymmetry and tail thickness, respectively. The higher order moments such as skewness and kurtosis could be calculated by the two parameters.

[1] This paper uses the normal inverse Gaussian (NIG) distribution which follows He and Hamori (2021).

In the ACD model, the dynamics for the two parameters can be modeled by the first-order quadratic-type dynamics:

$$\rho_t = \Phi\left(\bar{\rho}_{\mathrm{t}}\right) = L_{\bar{\rho}_{\mathrm{t}}} + \frac{(U_{\bar{\rho}_{\mathrm{t}}} - L_{\bar{\rho}_{\mathrm{t}}})}{1+e^{-\bar{\rho}_{\mathrm{t}}}},, \tag{2a}$$

$$\zeta_t = \Phi\left(\bar{\zeta}_{\mathrm{t}}\right) = L_{\bar{\zeta}_{\mathrm{t}}} + U_{\bar{\zeta}_{\mathrm{t}}} e^{-\upsilon\bar{\zeta}_{\mathrm{t}}}, \tag{2b}$$

$$\bar{\rho}_{\mathrm{t}} = a_0 + a_1 z_{t-1} + a_2 z_{t-1}^2 + c_1 \bar{\rho}_{\mathrm{t}-1}, \tag{2c}$$

$$\bar{\zeta}_{\mathrm{t}} = b_0 + b_1 z_{t-1} + b_2 z_{t-1}^2 + d_1 \bar{\zeta}_{\mathrm{t}-1}. \tag{2d}$$

Where $\bar{\rho}_{\mathrm{t}}$ and $\bar{\zeta}_{\mathrm{t}}$ are the unconstrained motion dynamics of the skew parameter ρ_t and ζ_t respectively. $\Phi(\cdot)$ represents an appropriate transformation function. L and U are the lower and upper bounds of the distributional parameters.

2.2. The Diebold–Yilmaz TVP-VAR-based Approach

In this research, a TVP-VAR with one lag will be employed based on the Schwartz information criterion (SC). Consider an N-variable TVP-VAR(1) model as follows:

$$\boldsymbol{y}_t = \boldsymbol{\Phi}_{1t}\boldsymbol{y}_{t-1} + \boldsymbol{\varepsilon}_t, \qquad \boldsymbol{\varepsilon_t}|\boldsymbol{\Omega}_{t-1} \sim \boldsymbol{N}(\boldsymbol{0}, \boldsymbol{\Sigma}_t), \tag{3a}$$

$$\mathrm{vec}(\boldsymbol{\Phi}_t) = \mathrm{vec}(\boldsymbol{\Phi}_{t-1}) + \boldsymbol{\eta}_t, \ \boldsymbol{\eta}_t|\boldsymbol{\Omega}_{t-1} \sim \boldsymbol{N}(\boldsymbol{0}, \boldsymbol{\Xi}_t), \tag{3b}$$

where $\boldsymbol{\Omega}_{t-1}$ represents all available information up to $t-1$, the endogenous variables $\boldsymbol{y}_t$ is an $N \times 1$ dimensional vector. $\boldsymbol{\Phi}_t$ is an $N \times N$ matrix and its vectorization $\mathrm{vec}(\boldsymbol{\Phi}_t)$ is an $N^2 \times 1$ vector. The shocks $\boldsymbol{\varepsilon}_t$ and $\boldsymbol{\eta}_t$ are $N \times 1$ and $N^2 \times 1$ dimensional vectors, respectively. Moreover, variance-covariance matrices $\boldsymbol{\Sigma}_t$ and $\boldsymbol{\Xi}_t$ are $N \times N$ and $N^2 \times N^2$ dimensional matrices, respectively.

According to the Wold representation theorem, we can transform the TVP-VAR into a TVP-VMA as follows:

$$\boldsymbol{y_t} = \sum_{j=1}^{\infty} \boldsymbol{\Lambda}_{jt} \boldsymbol{\varepsilon}_{t-j} + \boldsymbol{\varepsilon}_t. \tag{4}$$

We can then calculate the generalized forecast error variance decomposition (GFEVD), which was introduced by Koop et al. (1996), and Pesaran & Shin (1998), using TVP-VMA coefficients to compute the dynamic connectedness measures (Diebold & Yilmaz, 2009, 2012, 2014).

The H-step-ahead GFEVD under the generalized VAR framework can be expressed as follows:

$$\theta_{jk,t}^{H} = \frac{\Sigma_{kk,t}^{-1} \sum_{h=0}^{H-1} \left(e_j' \boldsymbol{\Lambda}_{h,t} \boldsymbol{\Sigma}_t e_k\right)^2}{\sum_{h=0}^{H-1} \left(e_j' \boldsymbol{\Lambda}_{h,t} \boldsymbol{\Sigma}_t \boldsymbol{\Lambda}_{h,t}' e_j\right)}, \tag{5}$$

where H is the forecast horizon that is set to 10 in this paper. e_i is a selection vector with one on the i−th position and zeros elsewhere. $\boldsymbol{\Lambda}_{h,t}$ represents the coefficient matrix multiplying the h-lagged shock vector in the TVP-VMA at time t, and $\Sigma_{kk,t}$ is the k-th diagonal element of the covariance matrix $\boldsymbol{\Sigma}_t$.

After the normalization, the pairwise connectedness index from the k−th variable to the j−th variable at horizon H at time t can be calculated by

$$\tilde{\theta}_{jk,t}^{H} = \frac{\theta_{jk,t}^{H}}{\sum_{k=1}^{N} \theta_{jk,t}^{H}}, \tag{6}$$

Meanwhile, the total connectedness index can be represented as

$$S_t^H = \frac{1}{N} \sum_{j,k=1, j \neq k}^{N} \tilde{\theta}_{jk,t}^H . \quad (7)$$

Moreover, the directional connectedness (From), which measures the averaged spillover to the k −th variable from all remaining variables in the system, can be calculated as

$$S_{k\leftarrow\cdot,t}^H = \frac{1}{N} \sum_{j=1, j \neq k}^{N} \tilde{\theta}_{kj,t}^H . \quad (8)$$

Similarly, the directional connectedness (To), which measures the total averaged spillover from the k −th variable to all the remaining variables in the system, can be calculated as

$$S_{\cdot\leftarrow k,t}^H = \frac{1}{N} \sum_{j=1, j \neq k}^{N} \tilde{\theta}_{jk,t}^H . \quad (9)$$

The above-defined measures of connectedness at time t are summarized in Table 1.

Table 1: Averaged Diebold–Yilmaz connectedness index table

	y_1	y_2	…	y_N	From
y_1	$\tilde{\theta}_{11}^H$	$\tilde{\theta}_{12}^H$	⋯	$\tilde{\theta}_{1N}^H$	$S_{1\leftarrow\cdot}^H$
y_2	$\tilde{\theta}_{21}^H$	$\tilde{\theta}_{22}^H$	⋯	$\tilde{\theta}_{2N}^H$	$S_{2\leftarrow\cdot}^H$
⋮	⋮	⋮	⋱	⋮	⋮
y_N	$\tilde{\theta}_{N1}^H$	$\tilde{\theta}_{N2}^H$	⋯	$\tilde{\theta}_{NN}^H$	$S_{N\leftarrow\cdot}^H$
To	$S_{\cdot\leftarrow 1}^H$	$S_{\cdot\leftarrow 2}^H$	⋯	$S_{\cdot\leftarrow N}^H$	S^H

Note: Adapted from (Diebold & Yilmaz, 2015).

2.3. Portfolio back-testing models

2.3.1 Minimum Connectedness Portfolio

In the spirit of the minimum variance portfolio and minimum correlation portfolio, (Broadstock et al., 2020) proposed the MCoP by using all Diebold-Yilmaz pairwise spillover indices instead of the variance or correlation matrix in the minimum variance portfolio or minimum correlation portfolio. By minimizing the interconnectedness and spillover effects among variables, a more resilient investment portfolio can be achieved, which is less susceptible to the adverse impacts of network shocks. Consequently, variables (investment instruments) that neither affect nor are influenced by others will receive higher weights within the portfolio. This can be expressed as follows:

$$\boldsymbol{\omega}_{Rt} = \frac{\boldsymbol{PCI}_t^{-1}\boldsymbol{I}}{\boldsymbol{IPCI}_t^{-1}\boldsymbol{I}}. \tag{10}$$

Where $\boldsymbol{PCI}_t$ is the pairwise connectedness index matrix, and $\boldsymbol{I}$ is the identity matrix.

2.3.2 Portfolio evaluation

To evaluate the effectiveness of the hedging and portfolio strategy, on the one hand, we calculate the hedge effectiveness as proposed by (EDERINGTON, 1979) which can be calculated as:

$$HE = 1 - \frac{Var(y_p)}{Var(y_{unhedged})}. \tag{11}$$

$Var(y_{unhedged})$ is the variance of the portfolio returns, and $Var(y_p)$ represents the variance of the un-hedged asset.

The hedge effectiveness reflects the percent reduction in the variance of the un-hedged position. The higher the hedge effectiveness the larger is the volatility risk reduction and vice versa. Following this line of thought, to measure the ability of the hedging portfolio to reduce extreme risks, we adapted Ederington's hedge efficiency for volatility risk, and calculated the hedge efficiency for VaR and for ES accordingly. The calculations are conducted as follows:

$$HE_{VaR} = 1 - \frac{VaR(y_p)}{VaR(y_{unhedged})}, \tag{12a}$$

$$HE_{ES} = 1 - \frac{CVar(y_p)}{CVar(y_{unhedged})}. \tag{12b}$$

Where HE_{VaR} and HE_{ES} are hedge efficiency for VaR and for ES, respectively.

On the other hand, we calculate the Sharpe ratio of return over volatility (SR), which proposed by Sharpe (1994), is calculated as follows.

$$SR = \frac{\bar{r}_p}{\sqrt{var(r_p)}}. \tag{13}$$

Where r_p is the portfolio returns assuming that the risk-free rate is equal to zero. In addition, similar to the hedge effectiveness, we also calculate the Sharpe ratios of return over VaR (SR_{VaR}) and ES (SR_{ES})[2] as follows.

$$SR_{VaR} = \frac{\bar{r}_p}{VaR(r_p)}, \tag{13a}$$

[2] The confidence levels for both VaR and ES are 95%, the same as that in hedge effectiveness.

$$SR_{ES} = \frac{\bar{r}_p}{CVaR(r_p)}. \tag{13b}$$

The SR, SR_{VaR}, and SR_{ES} indicate which portfolio has the highest return given the same volatility, VaR, and ES, respectively.

3. Data and Descriptive Statistics

At Binance, more than 350 cryptocurrencies are being traded. For this study, we have selected the top 9 cryptocurrencies with the highest market capitalization as of January 2023, excluding stablecoins such as Tether (USDT), USD Coin (USDC), and Binance USD (BUSD), which are highly pegged to the US dollar. The selected cryptocurrencies are Bitcoin (BTC), Binance Coin (BNB), Ethereum (ETH), XRP, Cardano (ADA), Dogecoin (DOGE), Polygon (MATIC), Polkadot (DOT), and Solana (SOL). As of January 2023, these 9 cryptocurrencies collectively account for over 65% of the total market. Our data covers the period from August 18, 2020, to January 1, 2023. We selected this time period for two reasons: firstly, the data for DOT and SOL became available only from August 2020 onwards, and secondly, prior to 2020, most cryptocurrencies experienced only minor fluctuations within a narrow price range. All the cryptocurrencies analyzed in this paper are spot trading pairs, and the data is sourced from Binance, with units denominated in USDT.

After obtaining the raw data for the cryptocurrencies, we calculate the returns for each trading pair using a logarithmic difference transformation. Then, we utilize the ACD-NIG model to estimate the conditional volatility, conditional skewness, and

conditional kurtosis series. Table 2 presents a range of summary statistics for all series. Regarding the return series, except for BTC, ETH, and SOL, the returns of all other cryptocurrencies exhibit a right-skewed distribution, indicating the potential for exceptionally high returns, albeit with a low probability. Additionally, all return series exhibit leptokurtosis, except for BTC and ADA, which display platykurtic and mesokurtic distributions, respectively. A leptokurtic distribution suggests that returns are prone to extreme values, both negative and positive, indicating a higher tail risk. The p-values of the Jarque and Bera (Jarque & Bera, 1980) normality test confirm that none of the return series follow a normal distribution. The unit root test conducted by Elliott et al. (1996) shows that all return series exhibit no unit root. The results of the Fisher & Gallagher (2012) weighted portmanteau test reveal the presence of ARCH/GARCH type effects in all return series. In terms of conditional volatility, conditional skewness, and conditional kurtosis, the results of the Jarque and Bera (Jarque & Bera, 1980) normality test indicate that they are also non-normally distributed. Furthermore, the results of the unit root test developed by Elliott et al. (1996) indicate the absence of unit roots in the data.

Table 2: Summary statistics

	BTC	BNB	ETH	XRP	ADA	DOGE	MATIC	DOT	SOL
Returns									
Mean	0.000	0.003	0.001	0.000	0.001	0.003	0.004	0.000	0.001
Variance	0.001	0.003	0.003	0.004	0.003	0.009	0.006	0.004	0.006
Skewness	−0.236	0.622	−0.413	0.15	0.255	5.977	0.969	0.233	−0.368
Ex.Kurtosis	2.713	14.491	3.791	12.538	3.000	92.500	6.057	7.532	6.019
JB	0.00	0.00	0.00	0.00	0.00	0.00	0.00	0.00	0.00
ERS	0.00	0.00	0.00	0.00	0.00	0.00	0.00	0.00	0.00
$\boldsymbol{Q^2(5)}$	0.02	0.00	0.00	0.00	0.00	0.03	0.00	0.00	0.00
Conditional Volatilities									
Mean	0.036	0.05	0.049	0.058	0.055	0.068	0.074	0.063	0.073
Variance	0.000	0.001	0.000	0.001	0.000	0.005	0.001	0.001	0.001
Skewness	0.754	3.494	2.217	2.467	1.576	7.603	2.226	2.023	3.008
Ex.Kurtosis	0.439	16.956	7.434	7.385	3.113	86.492	6.664	4.750	12.869
JB	0.00	0.00	0.00	0.00	0.00	0.00	0.00	0.00	0.00
ERS	0.00	0.00	0.00	0.00	0.00	0.00	0.00	0.00	0.00
Conditional Skewness									
Mean	−0.054	−0.227	−0.219	−0.042	0.063	0.541	0.44	0.115	0.132
Variance	0.285	0.37	0.196	0.659	0.149	1.498	1.031	0.475	0.378
Skewness	−2.966	0.414	−1.272	−0.745	−2.684	3.008	2.019	0.104	−2.524
Ex.Kurtosis	16.473	1.862	8.708	8.15	10.611	14.729	8.531	1.003	10.256
JB	0.00	0.00	0.00	0.00	0.00	0.00	0.00	0.00	0.00
ERS	0.00	0.00	0.00	0.00	0.00	0.00	0.00	0.00	0.00
Conditional Kurtosis									
Mean	4.646	4.379	2.492	6.278	3.059	11.756	5.733	3.825	2.944
Variance	8.249	0.902	2.426	24.117	0.432	161.686	72.043	1.572	3.518
Skewness	7.692	4.346	15.789	11.018	8.186	6.437	5.806	4.548	14.539
Ex.Kurtosis	85.111	27.302	355.963	195.264	75.619	49.152	37.385	34.845	286.902
JB	0.00	0.00	0.00	0.00	0.00	0.00	0.00	0.00	0.00
ERS	0.00	0.00	0.00	0.00	0.00	0.00	0.00	0.00	0.00

Note: The table presents the descriptive statistics includes the mean, variance, skewness, excess kurtosis, and the p-value of the test of Jarque and Bera (JB; 1987), the Elliott et al., (1996) unit root test. and the Fisher & Gallagher (2012) weighted portmanteau test with 5 lags.

4. Empirical Results and Discussion

4.1. Averaged dynamic spillovers

Let's begin by focusing on the averaged spillover measures. Tables 3, 4, and 5 present the averaged volatility spillovers, averaged skewness spillovers, and averaged kurtosis spillovers among the cryptocurrency markets, respectively. The values on the main diagonal of each table are not our main concern as they correspond to shocks within the same variable. Our interest lies in the off-diagonal values, which represent the interactions and spillovers between different markets. The last row and the last column in each table represent directional spillover (to) and directional spillover (from), respectively. They indicate the average spillover level from a specific market to all other markets and the average spillover level from all other markets to a specific market. Lastly, the value at the bottom right corner of each table represents the total spillover, indicating the overall spillover level of all markets. By comparing and analyzing the results of Tables 3, 4, and 5, we can draw the following key findings.

First, we observe that in the cryptocurrency markets, as the order of the moment increases, the total spillover decreases. The total volatility spillover among markets is the highest (64.11%), followed by the skewness spillover (59.27%), and the kurtosis spillover is the smallest (29.82%). This finding is consistent with the results of He & Hamori (2021).

Secondly, the spillovers from and to other cryptocurrencies vary across different moments for each cryptocurrency. For instance, in terms of volatility, BNB exhibits the

highest volatility spillover to other currencies, while ETH receives the highest volatility spillover. However, when it comes to skewness, ADA shows the highest skewness spillover to other currencies while also receiving the highest skewness spillover. In the case of kurtosis, BTC transmits the highest kurtosis spillover to other currencies, whereas ETH receives the highest kurtosis spillover. These findings imply that BNB, ADA, and BTC are likely to transfer the most volatility risk, downside (upside) risk, and tail risk to other markets, respectively. At the same time, ETH is likely to receive the most volatility risk and tail risk, while ADA is likely to receive the most downside (upside) risk. The transmission of volatility risk, downside (upside) risk, and tail risk among different cryptocurrency markets varies in magnitude and direction. This suggests that we can obtain unique information regarding the transmission of various types of risk from volatility spillover, skewness spillover, and kurtosis spillover. This information can enable more tailored risk management approaches, potentially enhancing the efficiency and effectiveness of investment strategies.

Table 3: Averaged dynamic volatility spillover index table

	BTC	BNB	ETH	XRP	ADA	DOGE	MATIC	DOT	SOL	From
BTC	33.46	10.87	12.52	5.97	6.75	9.10	7.53	7.31	6.49	7.39
BNB	10.15	33.13	8.94	8.32	6.46	9.23	8.13	7.98	7.66	7.43
ETH	11.06	11.41	27.00	6.11	7.43	11.84	6.79	8.86	9.51	8.11
XRP	7.05	8.56	7.42	40.80	6.16	10.33	6.52	6.85	6.30	6.58
ADA	6.41	8.96	12.81	8.58	28.39	11.82	7.07	8.01	7.96	7.96
DOGE	6.54	6.21	5.87	5.98	4.37	58.29	3.69	4.96	4.10	4.64
MATIC	9.37	12.20	11.43	6.72	6.88	9.27	29.64	6.74	7.73	7.82
DOT	6.97	9.33	8.13	6.60	7.29	6.02	5.89	41.82	7.95	6.46
SOL	5.35	12.12	10.61	8.99	8.04	8.53	7.30	8.60	30.47	7.73
To	6.99	8.85	8.64	6.36	5.93	8.46	5.88	6.59	6.41	64.11

Table 4: Averaged dynamic skewness spillover index table

	BTC	BNB	ETH	XRP	ADA	DOGE	MATIC	DOT	SOL	From
BTC	49.65	6.50	10.08	4.64	11.17	1.79	2.39	6.33	7.44	5.59
BNB	4.39	34.29	9.08	8.87	12.23	4.62	8.53	13.31	4.69	7.30
ETH	6.80	9.31	33.63	8.35	13.29	3.81	5.45	12.14	7.23	7.38
XRP	3.53	9.71	9.03	39.69	11.49	4.41	6.63	10.94	4.57	6.70
ADA	6.84	11.09	11.41	9.66	30.17	4.01	6.26	11.24	9.31	7.76
DOGE	2.03	7.24	7.60	6.76	6.20	54.90	5.19	7.56	2.52	5.01
MATIC	2.33	11.18	7.63	7.84	9.36	5.33	40.79	11.07	4.47	6.58
DOT	3.51	12.47	10.77	9.60	10.86	3.60	7.07	36.59	5.53	7.05
SOL	7.74	6.46	8.01	5.31	13.07	1.87	3.09	7.60	46.86	5.91
To	4.13	8.22	8.18	6.78	9.74	3.27	4.96	8.91	5.08	59.27

Table 5: Averaged dynamic kurtosis spillover index table

	BTC	BNB	ETH	XRP	ADA	DOGE	MATIC	DOT	SOL	From
BTC	72.53	0.54	9.45	5.68	0.49	1.69	4.64	2.92	2.06	3.05
BNB	1.65	66.81	0.60	0.51	13.81	2.94	3.75	6.04	3.90	3.69
ETH	10.65	0.61	62.00	4.32	0.12	9.44	4.54	5.64	2.69	4.22
XRP	6.08	0.72	5.38	73.95	0.14	3.13	6.49	2.57	1.54	2.89
ADA	0.37	13.72	0.11	0.10	70.21	3.23	0.38	6.29	5.59	3.31
DOGE	1.22	2.46	2.47	2.33	2.07	84.71	1.32	2.42	1.01	1.70
MATIC	7.80	3.34	10.26	5.68	0.34	3.34	64.09	3.15	2.00	3.99
DOT	3.29	5.25	4.87	2.38	5.46	1.48	2.91	68.84	5.53	3.46
SOL	8.08	4.14	2.69	1.38	6.15	0.88	1.87	6.32	68.51	3.50
To	4.35	3.42	3.98	2.49	3.18	2.90	2.88	3.93	2.70	29.82

4.2. Dynamic total spillovers

To investigate how the spillover effects evolve over time and how extreme events affect them, we will focus on the results of dynamic total spillovers. In addition, to better illustrate the results, we present in the topmost panel of Figure 1 a price chart over time for the S&P cryptocurrency top 10 equal weight index, which reflects the overall price movements of the top 10 ranked cryptocurrencies. The second to fourth panels from the top downward show the dynamic changes in total volatility spillover, total skewness spillover, and total kurtosis spillover, respectively.

To investigate the evolution of spillover effects over time and their response to extreme events, we focus on the dynamic total spillovers. To enhance the understanding of the results, Figure 1 presents a price chart for the S&P cryptocurrency top 10 equal weight index in the topmost panel. This index reflects the overall price movements of the top 10 ranked cryptocurrencies. The second to fourth panels, from top to bottom, display the dynamic changes in total volatility spillover, total skewness spillover, and total kurtosis spillover, respectively.

Analyzing Figure 1, let's first examine the overall trend of the cryptocurrency market from August 2020 to January 2023. As depicted in the figure, the cryptocurrency market has undergone an extended period of bullish behavior until May 2021, with prices steadily and significantly rising. However, from May to July 2021, the market experienced a sharp decline, with prices plummeting by over 50%. Subsequently, prices gradually recovered until approximately November 2021. However, starting from November 2021, the cryptocurrency market gradually entered another phase of decline,

characterized as a bear market. Overall, during this period, the cryptocurrency market has exhibited highly volatile and unpredictable behavior.

More specifically, prior to May 2021, the cryptocurrency market is characterized by a steady upward trend, during which the volatility spillover, skewness spillover, and kurtosis spillover exhibit a decreasing trend or remain at relatively low levels. On May 19th, 2021, the cryptocurrency market experiences a significant downturn, with major cryptocurrencies like Bitcoin and Ethereum plunging by over 30% within hours. This sudden crash is triggered by a combination of factors, including regulatory crackdowns on cryptocurrency exchanges and Tesla's announcement that it no longer accepts Bitcoin as payment. Subsequently, the volatility spillover experiences a sharp increase, while skewness spillover and kurtosis spillover steadily rise. From July to November 2021, the cryptocurrency market witnesses a price rebound. During this period, volatility spillover remains consistently high with minimal variation. In contrast, skewness spillover and kurtosis spillover exhibit a continuous and gradual increase. In October, this upward trend briefly pauses. However, following the resumption of the decline in cryptocurrency market prices after November, the skewness spillover and kurtosis spillover resume their steady rise. This rise persists until March 2023, spanning the entirety of the bear market.

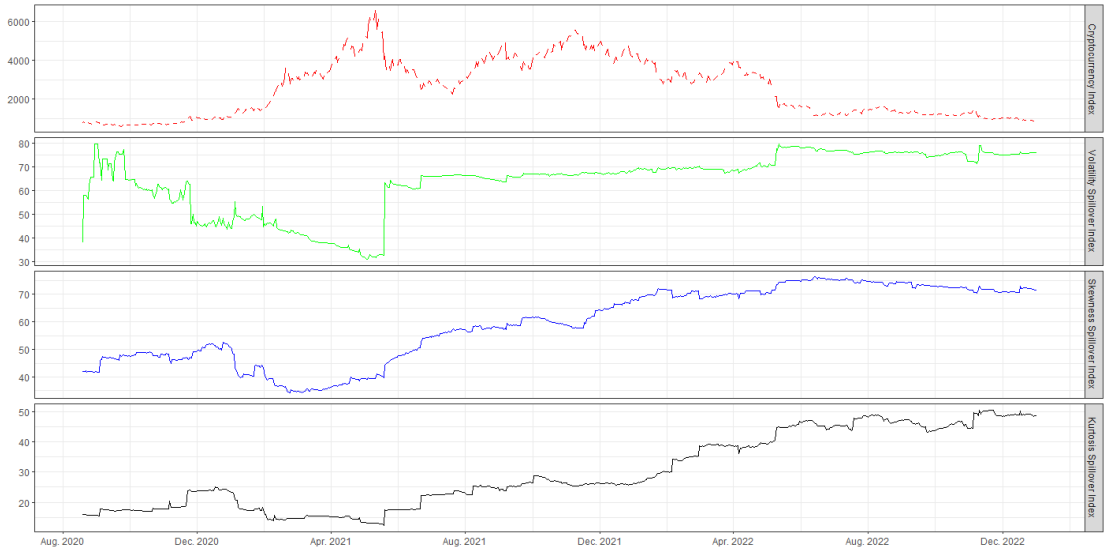

Fig.1: Cryptocurrency index and dynamic total spillovers

4.3. Portfolio and hedging strategies analysis

In this section, we present investment portfolios constructed using the MCoP (Minimum Connectedness Portfolio) based on the Diebold-Yilmaz connectedness index at different moments.

To provide a more concrete understanding of the composition of the individual portfolios, we illustrate the dynamic portfolio weights of the MCoP calculated based on the connectedness measures of different moments in Figures 2, 3, and 4, respectively.

By definition, the weights of the MCoP reflect the level of volatility connectedness (spillover) and aim to minimize the transmission of volatility risk across markets. Similarly, the weights of the MCoP for minimum kurtosis connectedness portfolios are determined by the level of kurtosis connectedness (spillover), with the objective of minimizing the transmission of tail risk across markets. Lastly, the weights of the MCoP for minimum skewness connectedness portfolios are determined by the size of

skewness connectedness (spillover) and serve the purpose of minimizing the transmission of downside (upside) risk across markets.

Based on Figures 2, 3, and 4, it is evident that the weight changes of portfolios based on skewness connectedness and those based on kurtosis connectedness exhibit similarities for certain cryptocurrencies. Specifically, prior to 2021, the portfolios' weights based on volatility connectedness undergo significant fluctuations. In contrast, the weight changes in portfolios based on skewness connectedness and kurtosis connectedness are relatively stable. Nevertheless, there are still notable differences in the weight changes across the three moments. These disparities arise due to variations in the dynamic spillovers of cryptocurrencies under different moments, despite some similarities in the dynamic changes of skewness spillover and kurtosis spillover. As the portfolio weights are determined by minimizing interconnectedness and spillover effects among the variables, assets that neither impact nor are influenced by others receive higher weights within the portfolio. Consequently, the weights assigned to each cryptocurrency adjust according to its dynamic spillover patterns.

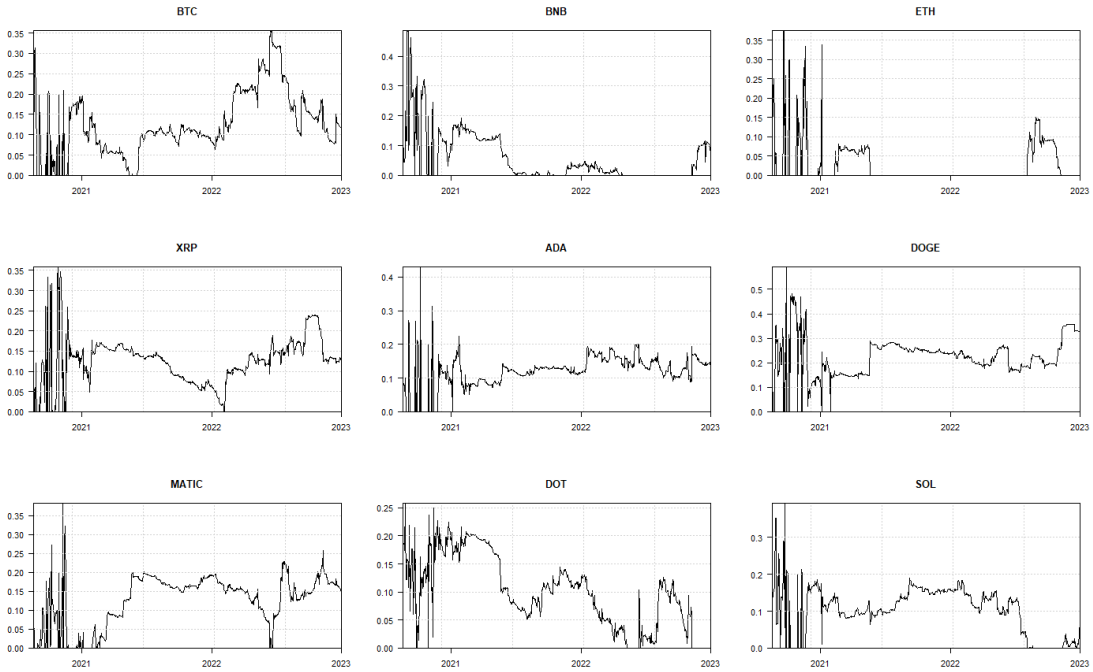

Fig.2: Dynamic multivariate portfolio weights: minimum volatility connectedness portfolio

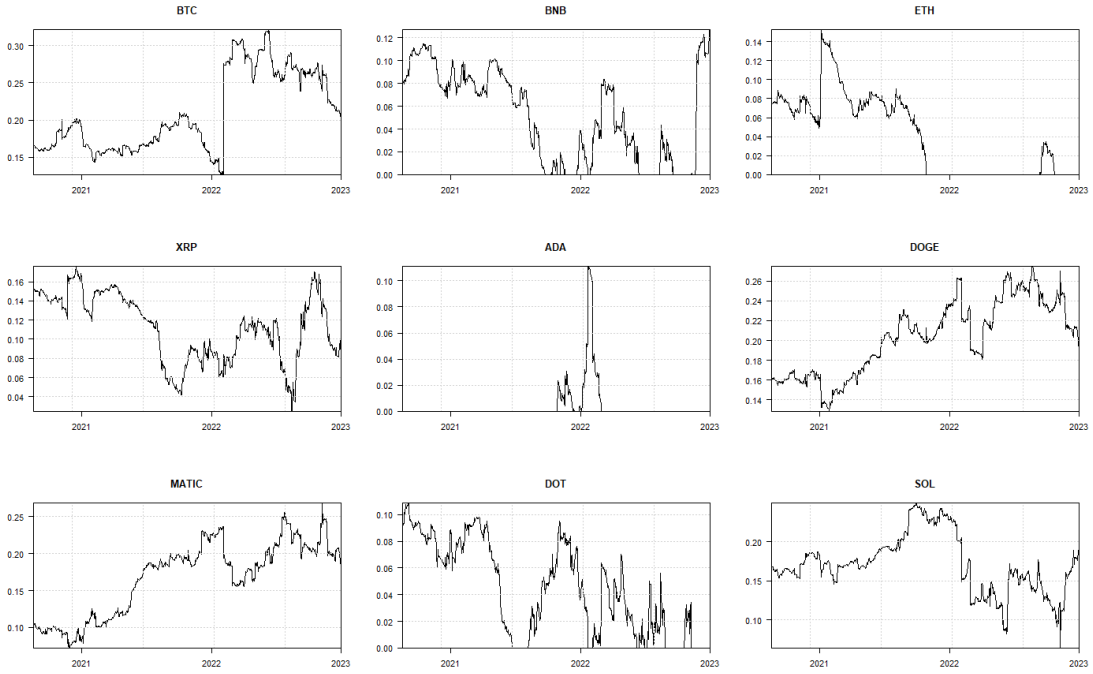

Fig.3: Dynamic multivariate portfolio weights: minimum skewness connectedness portfolio

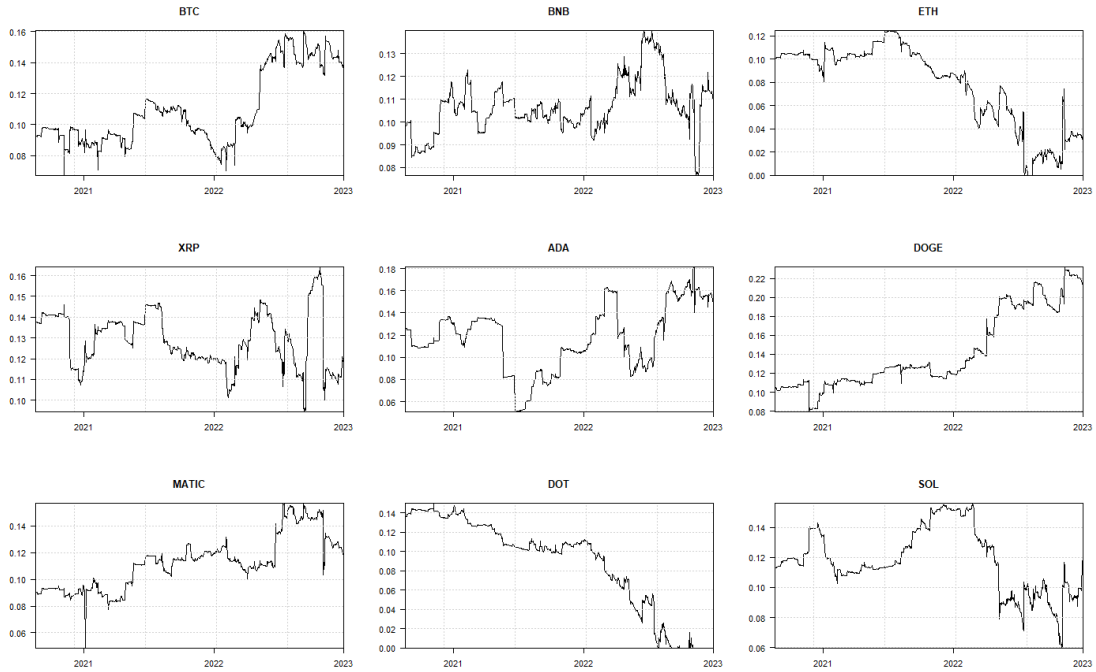

Fig.4: Dynamic multivariate portfolio weights: minimum kurtosis connectedness portfolio

In relation to the hedge effectiveness ratios presented in Table 6, the findings for the minimum volatility connectedness portfolio indicate that allocating an average of 12% to BTC, 6% to BNB, 3% to ETH, 13% to XRP, 12% to ADA, 22% to DOGE, 13% to MATIC, 10% to DOT, and 10% to SOL would lead to reductions in asset volatility of -102%, 15%, -9%, 37%, 19%, 70%, 56%, 37%, and 54%, respectively. Additionally, the Value at Risk (VaR) for each asset in this portfolio would decrease by -34%, -12%, -3%, 8%, 7%, 14%, 19%, 16%, and 23%, while the Expected Shortfall (ES) would decrease by -40%, 1%, -6%, 14%, 0%, 22%, 18%, 11%, and 28%. Comparing the three portfolios, it is evident that the MCoP based on skewness connectedness or kurtosis connectedness demonstrates enhanced hedge effectiveness in terms of volatility, VaR, and ES, compared to the MCoP based on volatility connectedness. Furthermore, the

minimum kurtosis connectedness portfolio exhibits superior performance, showcasing the highest hedge effectiveness in reducing volatility, VaR, and ES.

The findings for the minimum kurtosis connectedness portfolio suggest that by allocating an average of 11% to BTC, 11% to BNB, 8% to ETH, 13% to XRP, 12% to ADA, 14% to DOGE, 11% to MATIC, 9% to DOT, and 12% to SOL, the volatility of each asset in this portfolio would decrease by -83%, 23%, 1%, 43%, 27%, 73%, 60%, 43%, and 58% respectively. Similarly, the Value at Risk (VaR) of each asset in this portfolio would decrease by -28%, -7%, 2%, 13%, 11%, 18%, 23%, 20%, and 27%, while the Expected Shortfall (ES) would decrease by -36%, 2%, -3%, 17%, 3%, 24%, 21%, 14%, and 30%.

Our findings regarding the enhanced hedge effectiveness of the MCoP based on skewness connectedness or kurtosis connectedness are consistent with the research conducted by Cui and Maghyereh (2023) on realized skewness and realized kurtosis. In their study, the MCoP based on realized skewness or realized kurtosis also improved the hedge effectiveness of volatility. Furthermore, our study extends these findings by confirming that the hedge effectiveness of VaR and ES is also improved.

Additionally, it is worth noting that the volatility of dynamic portfolio weights in the MCoP based on skewness connectedness or kurtosis connectedness is lower compared to that in the MCoP based on volatility.

Finally, the Sharpe ratios for the three portfolios are presented in Table 7. Similar to hedge effectiveness, we found that compared to the MCoP based on volatility

connectedness, the MCoP based on skewness connectedness or kurtosis connectedness also exhibits enhanced Sharpe ratios for return over standard deviation, VaR, and ES. However, this time, it is the minimum skewness portfolio that demonstrates the best performance, rather than the minimum kurtosis portfolio.

Table 6: Averaged portfolio weights and hedge effectiveness

	Mean	Std.Dev.	5%	95%	HE	HE_{VaR}	HE_{ES}
Minimum volatility connectedness portfolio							
BTC	0.12	0.08	0.00	0.28	–1.02	–0.34	–0.40
BNB	0.06	0.08	0.00	0.19	0.15	–0.12	–0.01
ETH	0.03	0.06	0.00	0.13	–0.09	–0.03	–0.06
XRP	0.13	0.06	0.02	0.24	0.37	0.08	0.14
ADA	0.12	0.05	0.00	0.18	0.19	0.07	0.00
DOGE	0.22	0.08	0.12	0.36	0.70	0.14	0.22
MATIC	0.13	0.07	0.00	0.20	0.56	0.19	0.18
DOT	0.10	0.06	0.00	0.20	0.37	0.16	0.11
SOL	0.10	0.06	0.00	0.18	0.54	0.23	0.28
Minimum skewness connectedness portfolio							
BTC	0.21	0.05	0.15	0.30	–0.89	–0.32	–0.38
BNB	0.05	0.04	0.00	0.11	0.20	–0.10	0.00
ETH	0.04	0.04	0.00	0.12	–0.02	–0.01	–0.04
XRP	0.11	0.03	0.05	0.16	0.41	0.10	0.15
ADA	0.00	0.01	0.00	0.03	0.24	0.09	0.01
DOGE	0.20	0.04	0.15	0.26	0.72	0.15	0.23
MATIC	0.17	0.05	0.09	0.24	0.59	0.21	0.20
DOT	0.04	0.03	0.00	0.09	0.41	0.17	0.13
SOL	0.17	0.04	0.11	0.24	0.57	0.25	0.29
Minimum kurtosis connectedness portfolio							
BTC	0.11	0.02	0.08	0.15	**–0.83**	**–0.28**	**–0.36**
BNB	0.11	0.01	0.09	0.13	**0.23**	**–0.07**	**0.02**
ETH	0.08	0.04	0.01	0.12	**0.01**	**0.02**	**–0.03**
XRP	0.13	0.01	0.11	0.15	**0.43**	**0.13**	**0.17**
ADA	0.12	0.03	0.06	0.16	**0.27**	**0.11**	**0.03**
DOGE	0.14	0.04	0.10	0.22	**0.73**	**0.18**	**0.24**
MATIC	0.11	0.02	0.08	0.15	**0.60**	**0.23**	**0.21**
DOT	0.09	0.05	0.00	0.14	**0.43**	**0.20**	**0.14**
SOL	0.12	0.02	0.08	0.15	**0.58**	**0.27**	**0.30**

Note: The table presents the means (Mean), standard deviations (Std.Dev.), 5th percentiles (5%), 95th percentiles (95%) of dynamic portfolio weights, and hedge effectiveness in terms of volatility (HE), Value at Risk (HE_{VaR}), and expected shortfall (HE_{ES}).

Table 7: Sharpe Ratio

	SR	SR_{VaR}	SR_{ES}
$MCoP_{vol}$	0.028	0.017	0.008
$MCoP_{skew}$	**0.032**	**0.019**	**0.009**
$MCoP_{kurto}$	0.031	0.018	**0.009**

Note: The table presents the Sharpe ratios of return over standard deviation (SR), Value at Risk (SR_{VaR}), and expected shortfall (SR_{ES}). $MCoP_{vol}$, $MCoP_{skew}$, and $MCoP_{kurto}$ refer to the MCoP based on volatility, skewness, and kurtosis, respectively.

5. Conclusions and Discussions

In this study, we conduct a comprehensive analysis of nine major cryptocurrencies traded on Binance, focusing on the spillover effects of conditional volatility and conditional higher moments, including skewness and kurtosis. Our data span the period from August 18, 2020, to January 1, 2023. Here are some key findings and conclusions.

First, we find that volatility, skewness, and kurtosis spillovers exhibit distinct patterns across different moments, with the total spillover decreasing as the order of the moment increases. Each cryptocurrency manifests a unique pattern of risk transmission across these moments. For instance, BNB and BTC dominate in transmitting volatility and kurtosis, respectively, while ADA shows the highest skewness spillover transmitted to others. These findings imply that BNB, ADA, and BTC are likely to transfer the most volatility risk, downside (upside) risk, and tail risk to other markets, respectively. These findings may be particularly useful for investors in formulating accurate strategies to guard against specific types of risks. The differential risk transference characteristics of these cryptocurrencies can enable more tailored risk management approaches, potentially improving the efficiency and effectiveness of investment strategies.

Second, we also observe dynamic changes in spillover effects, which are influenced by the overall market conditions and extreme events. The changes in skewness and kurtosis spillovers display high similarity, implying a consistent pattern in the transmission of downside (upside) risk and tail risk across markets over time. The changes and fluctuations in downside (upside) risk and tail risk are notably different from the transmission patterns of volatility risk. These findings carry significant implications for investors and risk managers. By understanding the unique transmission patterns of different types of risks across the cryptocurrency markets, they can better design their investment strategies and risk management practices. For instance, if an investor is more concerned about tail risk (which involves the risk of extreme market movements), they might pay more attention to the changes in kurtosis spillover over time, given that it behaves differently from volatility spillover. This would enable them to better anticipate and hedge against tail risk. Moreover, the high degree of similarity in the changes of skewness and kurtosis spillovers indicates that downside (upside) risk and tail risk often change hand-in-hand. This can help investors improve their risk diversification strategies by simultaneously considering these two types of risks.

The study further examines and compares the performances of the MCoP based on volatility, skewness, and kurtosis spillovers. We find that compared to the MCoP based on volatility, the MCoP based on higher moments shows enhanced hedge effectiveness and higher Sharpe ratios for volatility, VaR, and ES. Specifically, our results reveal that the MCoP based on kurtosis connectedness offers the highest hedge effectiveness, while

the MCoP based on skewness connectedness offers the highest Sharpe ratios.

In conclusion, this study provides valuable insights into the dynamic spillover effects among cryptocurrencies and their implications for risk management and portfolio construction. The findings highlight the importance of considering higher moments like skewness and kurtosis, in addition to volatility, for effective risk management in the cryptocurrency market. Understanding the higher moment spillover effects across cryptocurrency markets can help investors determine the transmission mechanism of risk more comprehensively and understand how markets are linked by the level of asymmetry and tailedness of their returns, which relates to upside (downside) risks and tail risks. These insights not only offer fresh and helpful perspectives on hedging strategies but also enrich the knowledge required for effective portfolio diversification and the management of extreme risks. Future research could expand on these findings by exploring other portfolio techniques or hedging strategies based on higher moment connectedness or by incorporating data from other markets.

6. References

Abdullah, M., Chowdhury, M. A. F., & Sulong, Z. (2023). Asymmetric efficiency and connectedness among green stocks, halal tourism stocks, cryptocurrencies, and commodities: Portfolio hedging implications. *Resources Policy*, *81*, 103419. https://doi.org/10.1016/J.RESOURPOL.2023.103419

Adekoya, O. B., Akinseye, A. B., Antonakakis, N., Chatziantoniou, I., Gabauer, D., & Oliyide, J.

(2022). Crude oil and Islamic sectoral stocks: Asymmetric TVP-VAR connectedness and investment strategies. *Resources Policy*, *78*, 102877. https://doi.org/10.1016/J.RESOURPOL.2022.102877

Bouri, E., Lei, X., Jalkh, N., Xu, Y., & Zhang, H. (2021). Spillovers in higher moments and jumps across US stock and strategic commodity markets. *Resources Policy*, *72*, 102060. https://doi.org/10.1016/J.RESOURPOL.2021.102060

Broadstock, D. C., Chatziantoniou, I., & Gabauer, D. (2020). Minimum Connectedness Portfolios and the Market for Green Bonds: Advocating Socially Responsible Investment (SRI) Activity. *SSRN Electronic Journal*. https://doi.org/10.2139/SSRN.3793771

Cui, J., & Maghyereh, A. (2023). Higher-order moment risk connectedness and optimal investment strategies between international oil and commodity futures markets: Insights from the COVID-19 pandemic and Russia-Ukraine conflict. *International Review of Financial Analysis*, *86*, 102520. https://doi.org/10.1016/J.IRFA.2023.102520

Diebold, F. X., & Yilmaz, K. (2009). Measuring financial asset return and volatility spillovers, with application to global equity markets. *The Economic Journal*, *119*(534), 158–171.

Diebold, F. X., & Yilmaz, K. (2012). Better to give than to receive: Forecast-based measurement of volatility spillovers. *International Journal of Forecasting*, *28*(1), 57–66.

Diebold, F. X., & Yilmaz, K. (2014). On the network topology of variance decompositions: Measuring the connectedness of financial firms. *Journal of Econometrics*, *40*(2), 373–401.

Diebold, F. X., & Yilmaz, K. (2015). Financial and Macroeconomic Connectedness. In *Financial and Macroeconomic Connectedness*. Oxford University Press. https://doi.org/10.1093/acprof:oso/9780199338290.001.0001

EDERINGTON, L. H. (1979). The Hedging Performance of the New Futures Markets. *The Journal of Finance*, *34*(1), 157–170. https://doi.org/10.1111/J.1540-6261.1979.TB02077.X

Elliott, G., Rothenberg, T. J., & Stock, J. H. (1996). Efficient Tests for an Autoregressive Unit Root. *Econometrica*, *64*(4), 813. https://doi.org/10.2307/2171846

Finta, M. A., & Aboura, S. (2020). Risk premium spillovers among stock markets: Evidence from higher-order moments. *Journal of Financial Markets*, *49*, 100533. https://doi.org/10.1016/J.FINMAR.2020.100533

Fisher, T. J., & Gallagher, C. M. (2012). New weighted portmanteau statistics for time series goodness of fit testing. *Journal of the American Statistical Association*, *107*(498), 777–787. https://doi.org/10.1080/01621459.2012.688465/SUPPL_FILE/UASA_A_688465_SUP_25848856.ZIP

Gkillas, K., Bouri, E., Gupta, R., & Roubaud, D. (2022). Spillovers in Higher-Order Moments of Crude Oil, Gold, and Bitcoin. *The Quarterly Review of Economics and Finance*, *84*, 398–406. https://doi.org/10.1016/J.QREF.2020.08.004

Hansen, B. E. (1994). Autoregressive Conditional Density Estimation. *International Economic Review*, *35*(3), 705–730.

He, X., & Hamori, S. (2021). Is volatility spillover enough for investor decisions? A new viewpoint from higher moments. *Journal of International Money and Finance*, *116*, 102412. https://doi.org/10.1016/J.JIMONFIN.2021.102412

He, X., & Hamori, S. (2023). Different moments create different spillovers: A study of commodity markets. *Singapore Economic Review*, *https://Doi.Org/10.1142/S021759082350025X*. https://doi.org/10.1142/S021759082350025X

He, X., Takiguchi, T., Nakajima, T., & Hamori, S. (2020). Spillover effects between energies, gold, and stock: the United States versus China. *Energy & Environment*.

Jarque, C. M., & Bera, A. K. (1980). Efficient tests for normality, homoscedasticity and serial independence of regression residuals. *Economics Letters*, *6*(3), 255–259. https://doi.org/10.1016/0165-1765(80)90024-5

Koop, G., Pesaran, M. H., & Potter, S. M. (1996). Impulse response analysis in nonlinear multivariate models. *Journal of Econometrics*, *74*(1), 119–147.

Liu, T., & Hamori, S. (2020). Spillovers to Renewable Energy Stocks in the US and Europe: Are They Different? *Energies*, *13*(12), 3162. https://doi.org/10.3390/en13123162

Nekhili, R., & Bouri, E. (2023). Higher-order moments and co-moments' contribution to spillover analysis and portfolio risk management. *Energy Economics*, *119*, 106596. https://doi.org/10.1016/J.ENECO.2023.106596

Pesaran, H. H., & Shin, Y. (1998). Generalized impulse response analysis in linear multivariate models. *Economics Letters*, *58*(1), 17–29.

Sharpe, W. F. (1994). The Sharpe Ratio. *The Journal of Portfolio Management*, *21*(1), 49–58. https://doi.org/10.3905/JPM.1994.409501

Sun, G., Li, J., & Shang, Z. (2022). Return and volatility linkages between international energy markets and Chinese commodity market. *Technological Forecasting and Social Change*, *179*, 121642. https://doi.org/10.1016/J.TECHFORE.2022.121642

Tiwari, A. K., Aikins Abakah, E. J., Gabauer, D., & Dwumfour, R. A. (2021). Green Bond, Renewable Energy Stocks and Carbon Price: Dynamic Connectedness, Hedging and Investment Strategies during COVID-19 pandemic. *SSRN Electronic Journal*.

https://doi.org/10.2139/SSRN.3897284

Tiwari, A. K., Cunado, J., Gupta, R., & Wohar, M. E. (2018). Volatility spillovers across global asset classes: Evidence from time and frequency domains. *The Quarterly Review of Economics and Finance*, *70*(C), 194–202.

Zhang, H., Jin, C., Bouri, E., Gao, W., & Xu, Y. (2022). Realized higher-order moments spillovers between commodity and stock markets: Evidence from China. *Journal of Commodity Markets*, 100275. https://doi.org/10.1016/J.JCOMM.2022.100275